



HAL
open science

Combination of tissue and liquid biopsy molecular profiling to detect transformation to small cell lung carcinoma during osimertinib treatment

Julie A Vendrell, Xavier Quantin, Isabelle Serre, Jérôme Solassol

► **To cite this version:**

Julie A Vendrell, Xavier Quantin, Isabelle Serre, Jérôme Solassol. Combination of tissue and liquid biopsy molecular profiling to detect transformation to small cell lung carcinoma during osimertinib treatment. *Therapeutic Advances in Medical Oncology*, 2020, 12, 10.1177/1758835920974192. hal-03166712

HAL Id: hal-03166712

<https://hal.umontpellier.fr/hal-03166712>

Submitted on 11 Mar 2021

HAL is a multi-disciplinary open access archive for the deposit and dissemination of scientific research documents, whether they are published or not. The documents may come from teaching and research institutions in France or abroad, or from public or private research centers.

L'archive ouverte pluridisciplinaire **HAL**, est destinée au dépôt et à la diffusion de documents scientifiques de niveau recherche, publiés ou non, émanant des établissements d'enseignement et de recherche français ou étrangers, des laboratoires publics ou privés.



Distributed under a Creative Commons Attribution - NonCommercial 4.0 International License

Combination of tissue and liquid biopsy molecular profiling to detect transformation to small cell lung carcinoma during osimertinib treatment

Julie A. Vendrell , Xavier Quantin, Isabelle Serre and Jérôme Solassol

Abstract

Background: Histological transformation of advanced non-small cell lung cancer (NSCLC) to small cell lung cancer (SCLC) is one of the mechanisms of resistance to third-generation tyrosine kinase inhibitors (TKIs), such as osimertinib. This acquired TKI resistance is linked to the high degree of tumor heterogeneity and adaptive cellular signaling pathways, including epidermal growth factor receptor (*EGFR*)-dependent pathways, observed in NSCLC.

Methods: Here, we investigated a series of paired pre- and post-histological transformation biopsies obtained from three patients initially having a NSCLC with an *EGFR*^{activating} mutation treated with first-generation TKI, who then received osimertinib as second-line after *EGFR*^{T790M} resistance and, lastly, developed a histological transformation to SCLC. Both tissue and liquid biopsies were analyzed using large panel sequencing approaches at various time points to reconstruct the clonal evolutionary history of the tumor.

Results: Our complementary analysis of tumor tissue and circulating tumor DNA samples allowed us to better characterize the histological and molecular alterations associated with resistance to osimertinib. SCLC transformation was linked to the presence of several concomitant gene alterations, including *EGFR*, *TP53* and *RB1*, but also to specific signal bypass, such as *EGFR* and *MET* amplifications and activation of the PI3K/AKT/mTOR pathway.

Conclusion: Our report emphasizes the mutational landscape of SCLC histological transformation and highlights the importance of combining tissue and liquid biopsy profiling before and during osimertinib treatment to predict such histological transformation.

Keywords: circulating tumor DNA, EGFR TKI resistance, histological transformation, lung cancer, osimertinib

Received: 29 June 2020; revised manuscript accepted: 23 October 2020.

Introduction

In patients with non-small cell lung cancer (NSCLC), epidermal growth factor receptor (*EGFR*) mutations identify subgroups of patients with tumor showing higher sensitivity to tyrosine kinase inhibitors (TKIs), compared with patients with tumors harboring wild type *EGFR*. These TKIs include reversible first-generation *EGFR* TKIs (e.g. gefitinib¹ and erlotinib²) and second-generation irreversible TKIs (e.g. afatinib).³ In patients with advanced lung adenocarcinoma

harboring an activating *EGFR* mutation, TKIs improve overall survival.⁴ However, almost all patients develop resistance to *EGFR* TKIs within 12–18 months.^{1,5}

Among the different identified mechanisms of acquired resistance, the secondary missense T790M mutation (*EGFR*^{T790M}) in *cis* with a primary activating mutant *EGFR* allele leads to a reduction in TKI binding to *EGFR*, and has been detected in approximately half of patients.⁶ Tumor

Ther Adv Med Oncol

2020, Vol. 12: 1–10

DOI: 10.1177/
175883520974192

© The Author(s), 2020.
Article reuse guidelines:
sagepub.com/journals-
permissions

Correspondence to:
Jérôme Solassol
Laboratoire de Biologie
des Tumeurs Solides,
Hôpital Arnaud de
Villeneuve, CHU de
Montpellier, 371, avenue
du Doyen Gaston Giraud,
Montpellier cedex 5,
34295, France; IRCM,
INSERM, Univ Montpellier,
ICM, Montpellier, France
j-solassol@chu-montpellier.fr

Julie A. Vendrell
Laboratoire de Biologie
des Tumeurs Solides,
Département de
Pathologie et Oncobiologie,
CHU Montpellier, Univ
Montpellier, Montpellier,
France

Isabelle Serre
Laboratoire
d'Anatomopathologie,
Département de
Pathologie et Oncobiologie,
CHU Montpellier, Univ
Montpellier, Montpellier,
France

Xavier Quantin
IRCM, INSERM, Univ
Montpellier, ICM,
Montpellier, France

progression can also be caused by the bypass or the activation of alternative signaling pathways, such as the PI3K-AKT pathway through *MET* or *HER2* amplification.⁷ Finally, histological transformation of advanced NSCLC into small cell lung cancer (SCLC) or squamous cell carcinoma also has been described in ~5% of the patients, as a rare but specific mechanism of TKI resistance.⁸

New third-generation irreversible EGFR TKIs, such as osimertinib and olmutinib, have been developed to overcome acquired EGFR TKI resistance due to the *EGFR*^{T790M} mutation. These TKIs have significantly improved the clinical management and outcome of patients with advanced NSCLC. Osimertinib is more efficient than first-generation EGFR TKIs and has been recently approved as first-line treatment, emerging as the new standard of care for advanced NSCLC with mutated *EGFR*.⁹ Unfortunately, resistance to osimertinib has been described after a median response duration of 17 months.⁹ Different mechanisms of resistance development have been described, and depend on whether osimertinib is administered as first- or second-line therapy.¹⁰ For instance, histological transformation is more frequent in patients who received osimertinib as first-line than second-line treatment (15% versus 9%).^{10,11}

Little is known about the molecular mechanisms that drive histological transformation. Inactivation of RB1 and TP53 has been commonly reported in transformed SCLC samples,^{12,16,17} and has been suggested as a predictive biomarker of SCLC transformation.¹³ However, Niederst and colleagues reported that RB1 loss is a necessary, but not sufficient, event for the development of acquired resistance *via* SCLC transformation.¹⁴ Moreover, large-scale sequencing analyses allowed the detection of alterations in genes implicated in different pathways, particularly *PIK3CA*.¹²⁻¹⁴

Currently, liquid biopsy offers the possibility to detect *EGFR* activating mutations and acquired resistance *EGFR*^{T790M} mutation from circulating tumor DNA (ctDNA), considerably modifying the medical care of NSCLC patients. However, ctDNA analysis does not allow assessing histological changes,¹⁵ underlying the importance of performing tumor tissue biopsies for unraveling the mechanisms of resistance to osimertinib. Furthermore, the molecular mechanisms of resistance to osimertinib *via* histological transformation have been poorly investigated in paired tumor samples collected before and after osimertinib

treatment initiation. Here, we report a small case series of three SCLC phenotype transformations in *EGFR*-mutated NSCLC patients treated with osimertinib as second-line TKI. We prospectively collected pre- and post-histological transformation tissue and liquid biopsy samples and conducted a paired comparison of the mutation profiles using next-generation sequencing (NGS) approaches.

Methods

Patients and sample collection

Tissue and blood samples from three NSCLC patients followed at the University Hospital of Montpellier (France) were collected at different time-course treatment. This study was performed with approval from the Institutional Review Board of the Montpellier University Hospital (Approval number: 2020_09_202000581). An approved informed consent statement was acquired for all patients. Two tissue samples were analyzed per patient: one at cancer diagnosis and another after relapse under osimertinib treatment (diagnostic of the SCLC transformation). After standard pathological examination, tissue punches using a 1 mm needle or macrodissected 10- μ m thick section were performed from tumor paraffin blocks to increase the percentage of tumor cells in the sample. Medical records were reviewed to extract clinicopathological data, including sex, age, smoking status, diagnoses, therapeutic agents, and survival. Tumor progression was defined according to RECIST 1.1 criteria.¹⁶ Liquid biopsy samples were collected in cell-free DNA blood collection tubes (Streck, La Vista, NE, USA).

DNA extraction

DNA was extracted from tissue samples using the Maxwell[®] RSC DNA FFPE Kit (Promega, Madison, WI, USA) according to the manufacturer's recommendations. Cell-free DNA from blood samples was isolated using the QIAamp Circulating Nucleic Acid Kit (Qiagen, Hilden, Germany) and its integrity was checked using the D5000 ScreenTapes and a 4200 TapeStation instrument (Agilent Technologies, Santa Clara, CA, USA). DNA was quantified using the Qubit dsDNA BR Assay Kit and a Qubit Fluorometer (Thermo Scientific, Wilmington, DE, USA).

Tissue sample NGS analysis

Libraries were prepared using the Advanta Solid Tumor NGS Library Prep Assay with the

automated Juno™ system on integrated fluidic circuits (LP 8.8.6 IFC) (Fluidigm) following the manufacturer's procedure. The panel allows the detection of somatic mutations in 53 oncology-relevant genes (234 kb, 1508 assays, Supplemental Material Table S1 online). Briefly, the LP 8.8.6 IFCs were primed with 20 ng of DNA per sample and the PCR mix. After amplification, harvested samples were pooled, purified using AMPure XP beads (Beckman Coulter, Brea, CA, USA), and a second PCR was performed to integrate the sequencing adapters. Libraries were then quantified, normalized and pair-end sequenced on a NextSeq instrument (2 × 150 cycles, Illumina, San Diego, CA, USA). After sequencing, the generated FastQ files were automatically analyzed using a bioinformatic workflow managed by Jflow.¹⁷ Briefly, reads were trimmed with cutadapt (v.1.18),¹⁸ aligned to the human genome GRCh37 with BWA (version 0.7.17),¹⁹ and variant calling was performed using VarDict (version 1.6.0). Variants present in both libraries with a variant allele frequency >5% and a depth coverage ≥300× were then annotated with Variant Effect Predictor (version 94)²⁰ and reported. Variants with a frequency ≥1% in the population according to the Exome Aggregation Consortium, Exome Sequencing Project or 1000 Genomes Project databases were considered as polymorphisms and were excluded.

ctDNA NGS analysis

Libraries were prepared using the LiquidPlex™ 28-gene Kit (Supplemental Table S2; ArcherDX, Boulder, CO, USA) according to the manufacturer's instructions. The optimal input amount of double-stranded cell-free DNA was 50 ng. For samples yielding <50 ng of cell-free DNA, the entire amount was used for library preparation. Briefly, unamplified DNA molecules were ligated to adapters, unique molecule barcoding and a synthetic universal priming sequence to enable target enrichment using gene-specific primers. After purification using Agencourt® AMPure® XP beads, a second PCR reaction was performed. After another purification step, libraries were quantified using the KAPA Library Quantification Kit (Roche, Meylan, France) and a LC480 instrument (Roche), normalized, pooled to equimolar concentration, and pair-end sequenced on an NextSeq (Illumina) instrument. Results were analyzed using the Archer Analysis v.6.0.3.2 software.

Droplet digital PCR (ddPCR)

Forward and reverse gene-specific primers and fluorescent hydrolysis probes specific for the mutant or wild-type sequence were obtained from Bio-Rad (Hercules, CA, USA). Briefly, 5–20 ng of ctDNA was used per ddPCR reaction with the ddPCR Supermix (Bio-Rad). Samples were emulsified in an automated droplet generator (Bio-Rad) and amplified using the following cycling conditions: 95°C for 10 min; 40 cycles of 94°C for 30 s and 55°C for 1 min; and 98°C for 10 min. After amplification, the fluorescence signal of individual droplets was analyzed with a QX200 Droplet Reader and the QuantaSoft V.1.7.4 software by applying a correction based on the Poisson distribution to the number of positive droplets for mutant or wild-type DNA. The number of copies of the mutant allele were reported to the volume of plasma used for ctDNA isolation.

Results

Patients

Lung carcinoma [LC]1 patient. This 68-year-old Caucasian non-smoking woman, whose chest X-ray findings indicated a right upper lobe mass, had a T3N2M0 NSCLC (p63-negative, TTF-1-positive by immunohistochemistry) harboring the *EGFR*^{del19} mutation following bronchoscopy (Figures 1 and 2). The patient first received chemoradiotherapy with cisplatin/pemetrexed followed by surgical resection (right pneumectomy) with incomplete (R1) resection and presence of residual microscopic tumor fragments. Therefore, she received erlotinib (150 mg/day) for 24 months without signs of disease progression by computed tomography (CT) during the follow-up. After the diagnosis of a breast tumor treated by surgery and radiotherapy, erlotinib was interrupted and reintroduced 12 months later. Positron emission tomography-CT (PET-CT) imaging at month 60 after the lung cancer diagnosis showed an increase of the primary lung tumor mass and the presence of bone costal metastases. Liquid biopsy analysis revealed the acquisition of *EGFR*^{T790M} subclones (acquired resistance to erlotinib) (Figure 3). Second-line treatment with osimertinib (80 mg/day) was administered for 7 months until CT imaging revealed disease progression with the increase of a lesion in the right lung and the appearance of liver metastases. Analysis of the tumor tissue biopsy obtained by bronchoscopy showed histological transformation to SCLC that was confirmed by the strong positivity

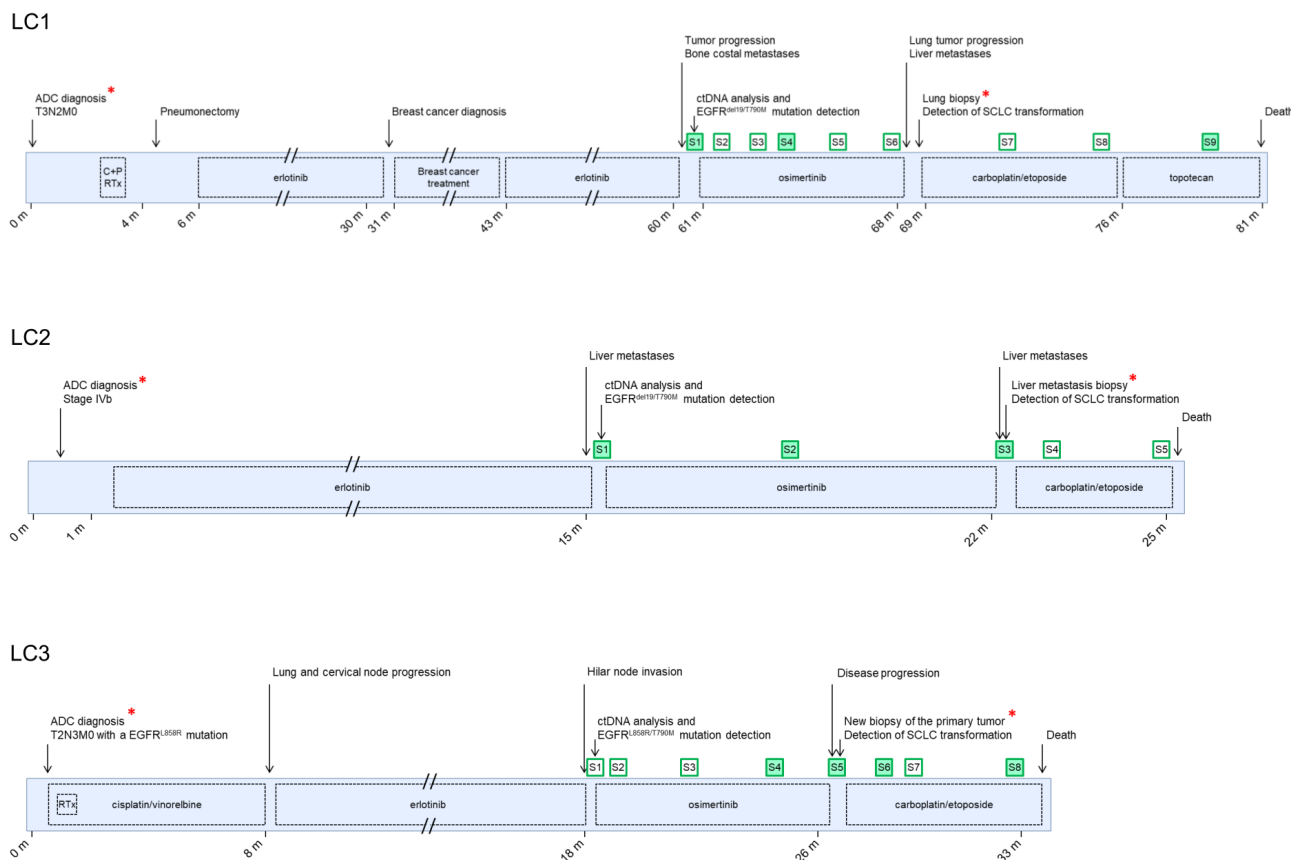


Figure 1. Graphical summary of the disease history of the three patients with lung carcinoma (LC). Treatments and clinical information are indicated. Red asterisks indicate tumor tissue biopsies analyzed by NGS; empty and filled green squares correspond to liquid biopsy samples analyzed by ddPCR and by both ddPCR and NGS, respectively. ADC, adenocarcinoma; C+P, cisplatin/pemetrexed; ddPCR, droplet digital PCR; m, months; NGS, next-generation sequencing; SCLC, small cell lung cancer; RTx, radiotherapy.

for CD56 and synaptophysin, moderate positivity for TTF-1 and low positivity for chromogranin A. The patient underwent chemotherapy with carboplatin/etoposide with a marked symptomatic improvement during the first cycle. After 7 months, due to disease progression, topotecan-based chemotherapy was introduced with partial response. The patient died 5 months later.

LC2 patient. A 71-year-old Caucasian woman (smoker) presented with back pain, and the CT scan showed a primary lung tumor in the apical segment of the right lobe associated with satellite lung nodules and mediastinal lymph nodes (Figure 1). Multiple bone lesions and infra-centimetric cerebral lesions were detected by PET-CT, and were confirmed by magnetic resonance imaging. The patient was staged IVb. Analysis of the endobronchial biopsy showed that the tumor was p63-negative and TTF-1-positive (immunohistochemistry) and

harbored the *EGFR*^{del19} mutation (Figure 2). The patient received erlotinib (150mg/day), but at month 15 after diagnosis, the follow-up CT screening revealed disease progression and the appearance of liver metastases. As ctDNA analysis showed the presence of the *EGFR*^{del19} and *EGFR*^{T790M} mutations (Figure 3), the patient was switched to osimertinib (80mg/day), which was well tolerated without need of dose reduction. CT screening at month 2 of osimertinib treatment demonstrated a partial response. However, 7 months after osimertinib initiation, hepatic metastases were detected by CT, and the serum level of the tumor marker neuron-specific enolase (NSE) increased to 37.1 ng/ml. Biopsy of one of the metastatic lesions led to the diagnosis of SCLC transformation, with persistence of the *EGFR*^{del19}, but not of the *EGFR*^{T790M} mutation (Figure 2). Osimertinib was stopped and replaced by carboplatin/etoposide. However, after two cycles, disease rapidly progressed with brain

| | LC1 | LC2 | LC3 | LC1 | LC2 | LC3 |
|--------------------------------|-----|-----|-----|-----|-----|-----|
| <i>EGFR</i> ^{del19} | 67 | 28 | | 58 | 35 | |
| <i>EGFR</i> ^{L858R} | | | 46 | | | 56 |
| <i>EGFR</i> ^{F180S} | 6 | | | | | |
| <i>TP53</i> ^{R248Q} | 35 | | | 43 | | |
| <i>TP53</i> ^{M246K} | | 32 | | | 95 | |
| <i>TP53</i> ^{L194R} | | | 41 | | | 66 |
| <i>RB1</i> ^{R787*} | | 22 | | | 60 | |
| <i>RB1</i> ^{Y325F} | | | 63 | | | 75 |
| <i>RB1</i> ^{Q504*} | | | 36 | | | 58 |
| <i>RICTOR</i> ^{R907C} | 51 | | | 45 | | |
| <i>PIK3CA</i> ^{E545K} | | | | 20 | | |
| <i>MET</i> ^{S213L} | | | 57 | | | 35 |
| <i>MET</i> ^{amp} | | | | | | 3 |

Figure 2. Alteration landscape of the paired tumor tissue biopsies collected before (yellow headings) and after histological transformation (green headings). The numbers in the boxes correspond to the variant allele frequency of the mutation or the gene copy number for amplifications. Samples were analyzed using the Advanta Solid Tumor NGS Library Prep Assay (Fluidigm) and sequenced on a NextSeq platform (Illumina). LC, lung carcinoma.

metastases, leading to the patient’s death 24 months after the initial diagnosis.

LC3 patient. This 77-year-old man, former smoker, with a T2N3M0 NSCLC harboring the *EGFR*^{L858R} mutation, and p63-negative/TTF-positive by immunohistochemistry (diagnosis made in an external center) (Figure 1), received radiotherapy and first-line cisplatin/vinorelbine. Follow-up CT screening demonstrated a partial response after three cycles with cervical node invasion and lung progression. The patient initiated treatment with erlotinib (150 mg/day), which led to a partial response after 3 months, followed by left hilar node invasion (CT imaging) after 10 months of treatment. Due to the detection of *EGFR*^{T790M} clones by ctDNA analysis (Figure 3), the patient was switched to osimertinib (80 mg/day), but disease progression was identified by CT screening after 7 months of treatment. A new biopsy of the primary tumor showed a SCLC

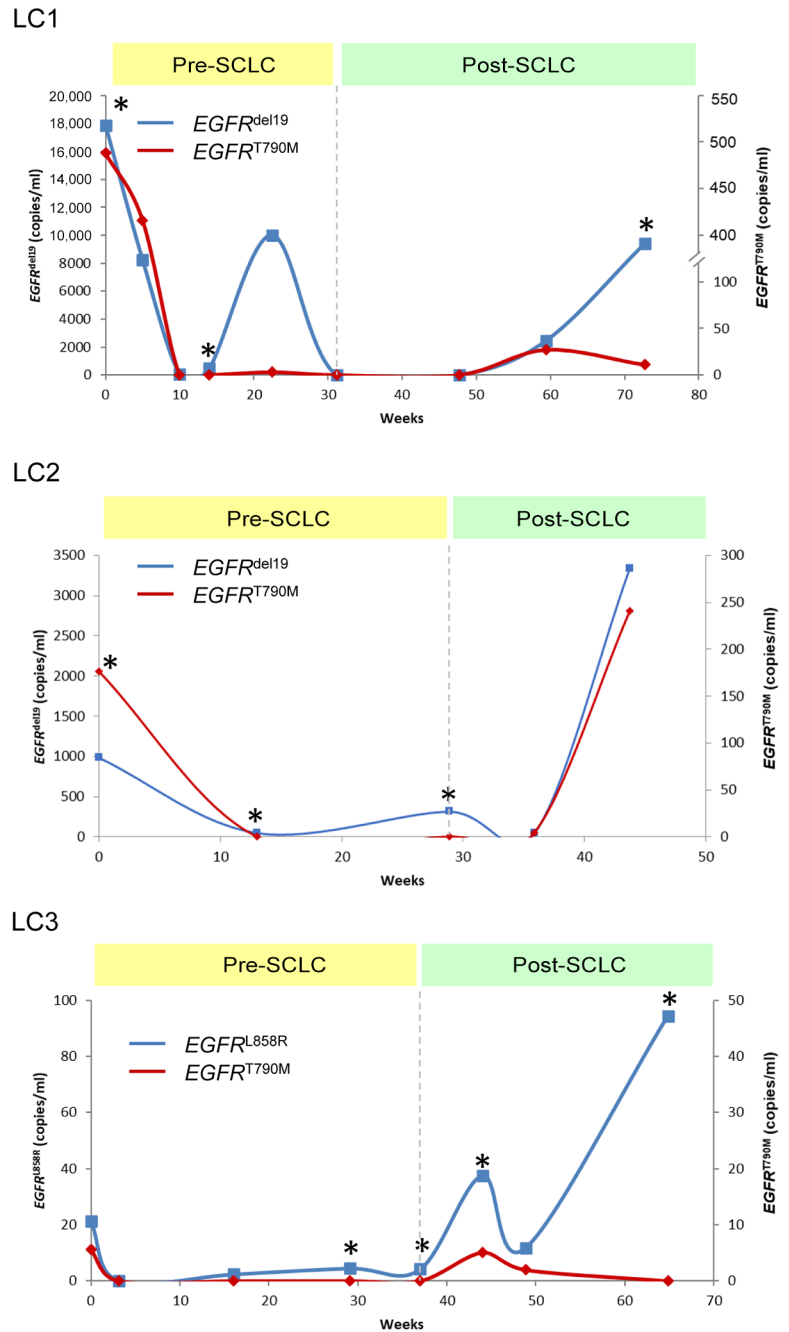


Figure 3. Monitoring of the *EGFR*^{activating} and *EGFR*^{T790M} alterations in circulating tumor DNA (ctDNA) samples collected before and after histological transformation. The levels of the *EGFR*^{del19} or *EGFR*^{L858R} (blue line) and *EGFR*^{T790M} (red line) mutations (copies/ml of plasma) were measured by droplet digital PCR. Asterisks indicated ctDNA samples analyzed by NGS. LC, lung carcinoma; NGS, next-generation sequencing; SCLC, small cell lung cancer.

component, characterized by positive staining for chromogranin A and synaptophysin, in association with a slight increase of NSE level in serum (19 ng/ml). The patient received four cycles of

| LC1 | | | | LC2 | | | | LC3 | | | | |
|--------------------------------|--------|--------|--------|------------------------------|--------|--------|--------|------------------------------|--------|--------|--------|--------|
| | LC1-S1 | LC1-S4 | LC1-S9 | | LC2-S1 | LC2-S2 | LC2-S3 | | LC3-S4 | LC3-S5 | LC3-S6 | LC3-S8 |
| <i>EGFR</i> ^{del19} | 88 | 30 | 82 | <i>EGFR</i> ^{del19} | 31 | 6 | 17 | <i>EGFR</i> ^{L858R} | 4 | 6 | 5 | 23 |
| <i>EGFR</i> ^{T790M} | 5.5 | | 0.2 | <i>EGFR</i> ^{T790M} | 8 | | | <i>EGFR</i> ^{T790M} | | | | 2 |
| <i>EGFR</i> ^{K728R} | 0.6 | | | <i>TP53</i> ^{M246K} | 22 | 6 | 24 | <i>EGFR</i> ^{L792H} | | | | 2 |
| <i>EGFR</i> ^{amp} | 8 | | 5.3 | | | | | <i>TP53</i> ^{L194R} | 3 | 6 | 4 | 21 |
| <i>PIK3CA</i> ^{E545K} | 10 | 6 | 29 | | | | | | | | | |
| <i>TP53</i> ^{R248Q} | 21 | 7 | 23 | | | | | | | | | |
| <i>MTOR</i> ^{R2322C} | | | 3 | | | | | | | | | |

Figure 4. Molecular alterations detected by NSG in liquid biopsy samples collected before (yellow) and after histological transformation (green). The number in the boxes corresponds to the variant allele fraction of the mutation or the gene copy number for amplifications. Samples were analyzed using the LiquidPlex™ 28-Gene Kit (ArcherDx) and sequenced on a NextSeq platform (Illumina). LC, lung carcinoma; NGS, next-generation sequencing.

carboplatin/etoposide chemotherapy to target the SCLC sub-population. After the initial clinical and radiological improvement, disease progressed with the development of brain metastases and the patient died 33 months after the initial diagnosis.

Tumor tissue and liquid biopsy molecular profiling

For each patient, paired tumor tissue samples collected at cancer diagnosis and at SCLC transformation after osimertinib treatment were analyzed by NGS (Figure 2). Interestingly, the *EGFR*^{activating} mutation present at diagnosis in all patients was conserved in the post-transformation tumor samples. *TP53* mutations were detected in all patients in paired samples, with a higher variant allele frequency in the SCLC samples. Nonsense mutations in *RBI1*, another gene frequently altered in the SCLC cell component, were detected in two patients (LC2 and LC3) at diagnosis and also after transformation. Overall, few mutations were detected only in one of the two paired samples. In patient LC1, the *EGFR*^{F180S} mutation was present only in the tumor sample at diagnosis, and the *PIK3CA*^{E545K} mutation only in the post-transformation biopsy. In patient LC3, a *MET* amplification, detected by NGS and validated by ddPCR (Figure 2 and Supplemental Figure S1), was detected only in the post-transformation sample.

For each patient, ctDNA samples were collected at different points during osimertinib treatment (Figure 1). Detection of the *EGFR*^{activating} and the *EGFR*^{T790M} mutations was performed by

ddPCR to monitor the patients' response to osimertinib (Figure 3). After treatment initiation, the number of copies of both mutant alleles rapidly decreased and remained very low or undetectable at the time of histological transformation diagnosis. After several weeks post-SCLC, the *EGFR*^{activating} mutation could be still detected in all three patients, whereas the *EGFR*^{T790M} mutation was found only in patient LC2. Some ctDNA samples were also analyzed by NGS (Figure 4) and the results revealed a good concordance with the data obtained from the matched tissue tumor samples. Indeed, the *EGFR*^{activating} mutation, *TP53* alterations, and *PIK3CA*^{E545K} mutation were similarly detected by the two approaches. In patient LC1, ctDNA analysis by NGS also allowed the detection of an *EGFR* amplification and a *MTOR*^{R2322C} mutation that were not targeted by the NGS panel used for tumor tissue samples.

Discussion

Although histological transformation is a well described NSCLC strategy of resistance to EGFR TKIs, the specific mechanisms involved are unclear. It has been hypothesized that a SCLC component already exists in the tumor before EGFR TKI treatment and that it progressively emerges due to the sensitivity of the predominant NSCLC component to EGFR TKIs.¹³ However, based on the observation that SCLC-transformed tumors still harbor the original activating *EGFR* mutations,^{6,14,21–26} trans-differentiation of advanced NSCLC to SCLC under the selective TKI pressure may also be hypothesized. In the present

study, the *EGFR*^{activating} mutation detected at diagnosis was maintained after the histological switch in all three patients, highlighting that NSCLC and SCLC share the same clonal origin. However, the *EGFR*^{T790M} mutation that was the mechanism of resistance developed by the three patients to first-line TKI treatment was not present in the SCLC cellular components analyzed by NGS, indicating that these cells probably emerged from a different cellular clone. However, ctDNA samples analyzed by ddPCR and NGS allowed the detection of the *EGFR*^{T790M} mutation also after SCLC transformation, suggesting the presence of focal metastatic sites still harboring this mutation, as reported by others.^{13,27}

To reconstruct the clonal tumor evolution, the determination of the concomitant genomic alterations linked to the histological transformation could be useful. Genome analysis by whole genome sequencing may be a powerful tool to establish the mutational landscape involved in SCLC transformation. However, due to the limited number of patients who developed this mechanism of resistance to EGFR TKIs and the scarcity of the available biopsy material, such analysis has only been performed by Lee *et al.* to our knowledge. These authors reported in four patients that the TKI-resistant SCLC clones can be derived from divergent evolutionary processes from adenocarcinoma at early stages.¹³ Moreover they suggested that the complete inactivation of RB1 and TP53 is a predictive biomarker of SCLC transformation.¹³ Using NGS approaches, *TP53* alteration was detected in 41% to 61% of patients with EGFR-mutated NSCLC and was associated with reduced response to EGFR TKIs and poor patient outcome.^{28–30} However, in these studies, the mechanisms of resistance in EGFR/TP53 co-mutated NSCLC were not investigated. Recently, Ferrer and colleagues reported that SCLC transformation occurs significantly earlier in EGFR-mutated than in non-EGFR-mutated NSCLC, although overall survival and response to treatment after transformation are similar between groups.³¹ Additional studies are needed to determine the relationship between *TP53* mutations, histological transformation, and patient clinical outcome.

In our study, the mutational status in paired pre- and post-transformation tissue biopsies and in sequential ctDNA samples was determined by NGS. Although the interval between tumor biopsies was quite long (69 months for patient LC1),

the mutational profile of paired tissue samples only slightly changed after SCLC transformation. Missense *TP53* alterations that are reported in the IARC *TP53* database to induce a non-functional protein were detected in the primary tumor of all three patients and their allele frequency was increased in the post-transformation biopsy. These *TP53* mutations were also detected in the ctDNA samples collected after SCLC transformation and analyzed by NGS. The *RBI*^{R787*} and *RBI*^{Q504*} nonsense mutations (previously observed in SCLC samples^{24,32}) were present in the paired tumor tissue samples of patients LC2 and LC3, respectively. As intronic mutations, chromosomal rearrangements or loss of heterozygosity are frequent events reported to induce Rb1 inactivation^{12,33} one could not exclude that LC1 samples harbored one of these alterations, which are not detectable by our NGS panels. Rb1 expression analysis by immunohistochemistry might have brought some information on this issue but, unfortunately, no tissue was left.

Our complementary analysis of tumor tissue and ctDNA samples by NGS showed the presence of gene alterations acquired during tumor progression. In patient LC1, SCLC transformation might be linked to the alteration of the PI3K/AKT/mTOR pathway, which is considered a core component of the histological transformation and a chemotherapy resistance mechanism in SCLC.^{12,34,35} Indeed, the *RICTOR*^{R907C} mutation was detected in the primary tumor and conserved in the SCLC sample. This mutation was not targeted by the NGS panel used for ctDNA analysis. The *PIK3CA*^{E545K} mutation was detected only in the post-transformation tumor biopsy and in ctDNA samples collected after treatment with erlotinib. Our analysis also allowed detecting the late acquisition of the *MTOR*^{R2322C} mutation. Moreover, the analysis of the different tumor tissue/ctDNA samples of patient LC1 suggested the presence of other tumoral subclones. Indeed, the *EGFR*^{F180S} mutation was detected only in the tumor biopsy at diagnosis, suggesting sensitivity of this clone to first-line TKI treatment. Acquisition of resistance to erlotinib was associated with the emergence of the *EGFR*^{T790M} mutation, which has been linked to focal amplification of *EGFR*.³⁶ Analysis of the sequential ctDNA samples showed that this subclone was first sensitive to second-line EGFR TKI treatment, as indicated by disappearance of the *EGFR*^{T790M} mutation. This mutation was detected again in ctDNA samples after SCLC transformation, but

not in the second tumor biopsy, possibly due to proliferation of *EGFR*^{T790M}-positive NSCLC cells at a metastatic site. In patient LC3, a *MET* amplification was detected only in the tumor biopsy after SCLC transformation. Moreover, the co-detection in a ctDNA sample of the *EGFR*^{T790M} mutation and the *EGFR*^{L792H} in *trans* suggests the presence of other tumor clones.

To conclude, this study brings some insights into the molecular mechanisms involved in SCLC transformation. To our knowledge, this is the first study that included pre- and post-SCLC transformation tumor biopsies and sequential ctDNA samples that were analyzed by NGS with the aim to determine the mutational profile during tumor treatment and progression. It also demonstrated the feasibility of using NSG and ctDNA samples to detect gene amplifications, a mechanism frequently reported in osimertinib resistance.¹¹

This observational study has some limitations. First, the number of patients was very small ($N=3$). Moreover, all three patients received osimertinib as second-line therapy after tumor relapse during treatment with erlotinib. Recent results from the FLAURA trial⁹ demonstrated that in patients with EGFR-mutated advanced NSCLC, front-line osimertinib provides a significant and clinically meaningful improvement in overall survival compared with the standard EGFR TKIs. Therefore, future studies should compare the molecular profile of histological transformation after osimertinib as first-line and later-line treatment. Moreover, not all ctDNA samples could be analyzed by NSG and, thus, the data obtained were not completely comparable to those obtained from tissue samples. Nevertheless, our results highlight the high intra-tumor heterogeneity and the acquisition of different molecular alterations that hinder EGFR TKI efficacy, as previously reported.^{12,23,36–38}

On the basis of the current knowledge and reported cases, we think that neither liquid biopsy nor solid biopsy on their own allows the exhaustive monitoring of cancer response to therapy. Although liquid biopsy is a non-invasive method with high informative value, histopathological analysis of tumor tissue remains the most relevant approach to identify histological transformation after acquired resistance to EGFR TKIs.¹⁵ However, the early detection of alterations in core genes (*TP53*, *RB1*, *PIK3CA*) might predict

histological transformation. Finally, given the heterogeneity of resistance mechanisms to third-generation TKIs, we think that analysis of a new tumor biopsy after disease progression during treatment with osimertinib remains crucial for understanding tumor biology, whereas ctDNA analysis by NGS can be proposed to assess tumor heterogeneity and to monitor tumor progression.

Acknowledgements

The authors thank the patients, donors, and their kin for agreement to publication of the report.

Author contributions

J.V. and J.S. conceived the study, J.V. and J.S. analyzed and interpreted the data and co-wrote the manuscript. X.Q., I.S. and J.S. were responsible for the clinical care of patients. All authors read and approved the final submitted version of the manuscript.

Availability of data and materials

The datasets generated and/or analyzed during this study are available from the corresponding author upon reasonable request.

Conflict of interest statement

The authors declare that there is no conflict of interest.

Ethics statement

The protocol was approved by Clinical Research Department of the university hospital (CRB-CHUM) of the principal investigator (J.S.) and was in accordance with the Declaration of Helsinki.

Funding

The authors received no financial support for the research, authorship, and/or publication of this article.

Informed consent

Written informed consent was obtained from the patients for publication of case reports.

ORCID iD

Julie A. Vendrell  <https://orcid.org/0000-0002-2071-6634>

Supplemental material

Supplemental material for this article is available online.

References

1. Mok TS, Wu YL, Yu CJ, *et al.* Randomized, placebo-controlled, phase II study of sequential erlotinib and chemotherapy as first-line treatment for advanced non-small-cell lung cancer. *J Clin Oncol* 2009; 27: 5080–5087.
2. Rosell R, Carcereny E, Gervais R, *et al.* Erlotinib versus standard chemotherapy as first-line treatment for European patients with advanced EGFR mutation-positive non-small-cell lung cancer (EURTAC): a multicentre, open-label, randomised phase 3 trial. *Lancet Oncol* 2012; 13: 239–246.
3. Yang JC, Wu YL, Schuler M, *et al.* Afatinib versus cisplatin-based chemotherapy for EGFR mutation-positive lung adenocarcinoma (LUX-Lung 3 and LUX-Lung 6): analysis of overall survival data from two randomised, phase 3 trials. *Lancet Oncol* 2015; 16: 141–151.
4. Zhou C, Wu YL, Chen G, *et al.* Final overall survival results from a randomised, phase III study of erlotinib versus chemotherapy as first-line treatment of EGFR mutation-positive advanced non-small-cell lung cancer (OPTIMAL, CTONG-0802). *Ann Oncol* 2015; 26: 1877–1883.
5. Ohashi K, Maruvka YE, Michor F, *et al.* Epidermal growth factor receptor tyrosine kinase inhibitor-resistant disease. *J Clin Oncol* 2013; 31: 1070–1080.
6. Hidaka N, Iwama E, Kubo N, *et al.* Most T790M mutations are present on the same EGFR allele as activating mutations in patients with non-small cell lung cancer. *Lung Cancer* 2017; 108: 75–82.
7. Wu SG and Shih JY. Management of acquired resistance to EGFR TKI-targeted therapy in advanced non-small cell lung cancer. *Mol Cancer* 2018; 17: 38.
8. Oser MG, Niederst MJ, Sequist LV, *et al.* Transformation from non-small-cell lung cancer to small-cell lung cancer: molecular drivers and cells of origin. *Lancet Oncol* 2015; 16: e165–e172.
9. Soria JC, Ohe Y, Vansteenkiste J, *et al.* Osimertinib in untreated EGFR-mutated advanced non-small-cell lung cancer. *N Engl J Med* 2018; 378: 113–125.
10. Schoenfeld AJ, Chan JM, Kubota D, *et al.* Tumor analyses reveal squamous transformation and off-target alterations as early resistance mechanisms to first-line osimertinib in EGFR-mutant lung cancer. *Clin Cancer Res* 2020; 26: 2654–2663.
11. Mehlman C, Cadranel J, Rousseau-Bussac G, *et al.* Resistance mechanisms to osimertinib in EGFR-mutated advanced non-small-cell lung cancer: a multicentric retrospective French study. *Lung Cancer* 2019; 137: 149–156.
12. Marcoux N, Gettinger SN, O'Kane G, *et al.* EGFR-mutant adenocarcinomas that transform to small-cell lung cancer and other neuroendocrine carcinomas: clinical outcomes. *J Clin Oncol* 2019; 37: 278–285.
13. Lee JK, Lee J, Kim S, *et al.* Clonal history and genetic predictors of transformation into small-cell carcinomas from lung adenocarcinomas. *J Clin Oncol* 2017; 35: 3065–3074.
14. Niederst MJ, Sequist LV, Poirier JT, *et al.* RB loss in resistant EGFR mutant lung adenocarcinomas that transform to small-cell lung cancer. *Nat Commun* 2015; 6: 6377.
15. Minari R, Bordi P, Del Re M, *et al.* Primary resistance to osimertinib due to SCLC transformation: issue of T790M determination on liquid re-biopsy. *Lung Cancer* 2018; 115: 21–27.
16. Eisenhauer EA, Therasse P, Bogaerts J, *et al.* New response evaluation criteria in solid tumours: revised RECIST guideline (version 1.1). *Eur J Cancer* 2009; 45: 228–247.
17. Mariette J, Escudie F, Bardou P, *et al.* Jflow: a workflow management system for web applications. *Bioinformatics* 2016; 32: 456–458.
18. Martin M. Cutadapt removes adapter sequences from high-throughput sequencing reads. *EMBnet J* 2011; 17: 10.
19. Li H and Durbin R. Fast and accurate short read alignment with Burrows-Wheeler transform. *Bioinformatics* 2009; 25: 1754–1760.
20. McLaren W, Gil L, Hunt SE, *et al.* The ensembl variant effect predictor. *Genome Biol* 2016; 17: 122.
21. Xu Y, Huang Z, Gong L, *et al.* A case of resistance to tyrosine kinase inhibitor therapy: small cell carcinoma transformation concomitant with plasma-genotyped T790M positivity. *Anticancer Drugs* 2017; 28: 1056–1061.
22. Fallet V, Ruppert AM, Poulot V, *et al.* Secondary resistance to erlotinib: acquired T790M mutation and small-cell lung cancer transformation in the same patient. *J Thorac Oncol* 2012; 7: 1061–1063.
23. Suda K, Murakami I, Yu H, *et al.* Heterogeneity in immune marker expression after acquisition of resistance to EGFR kinase inhibitors: analysis of a case with small cell lung cancer transformation. *J Thorac Oncol* 2017; 12: 1015–1020.
24. Morinaga R, Okamoto I, Furuta K, *et al.* Sequential occurrence of non-small cell and small cell lung cancer with the same EGFR mutation. *Lung Cancer* 2007; 58: 411–413.

25. Popat S, Wotherspoon A, Nutting CM, *et al.* Transformation to “high grade” neuroendocrine carcinoma as an acquired drug resistance mechanism in EGFR-mutant lung adenocarcinoma. *Lung Cancer* 2013; 80: 1–4.
26. Zakowski MF, Ladanyi M, Kris MG, *et al.* EGFR mutations in small-cell lung cancers in patients who have never smoked. *N Engl J Med* 2006; 355: 213–215.
27. Suda K, Murakami I, Sakai K, *et al.* Small cell lung cancer transformation and T790M mutation: complimentary roles in acquired resistance to kinase inhibitors in lung cancer. *Sci Rep* 2015; 5: 14447.
28. Labbe C, Cabanero M, Korpanty GJ, *et al.* Prognostic and predictive effects of TP53 co-mutation in patients with EGFR-mutated non-small cell lung cancer (NSCLC). *Lung Cancer* 2017; 111: 23–29.
29. Hou H, Qin K, Liang Y, *et al.* Concurrent TP53 mutations predict poor outcomes of EGFR-TKI treatments in Chinese patients with advanced NSCLC. *Cancer Manag Res* 2019; 11: 5665–5675.
30. Roeper J, Falk M, Chalaris-Rissmann A, *et al.* TP53 co-mutations in EGFR mutated patients in NSCLC stage IV: a strong predictive factor of ORR, PFS and OS in EGFR mt+ NSCLC. *Oncotarget* 2020; 11: 250–264.
31. Ferrer L, Giaj Levra M, Brevet M, *et al.* A brief report of transformation from NSCLC to SCLC: molecular and therapeutic characteristics. *J Thorac Oncol* 2019; 14: 130–134.
32. Zehir A, Benayed R, Shah RH, *et al.* Mutational landscape of metastatic cancer revealed from prospective clinical sequencing of 10,000 patients. *Nat Med* 2017; 23: 703–713.
33. Wagner AH, Devarakonda S, Skidmore ZL, *et al.* Recurrent WNT pathway alterations are frequent in relapsed small cell lung cancer. *Nat Commun* 2018; 9: 3787.
34. Lin MW, Su KY, Su TJ, *et al.* Clinicopathological and genomic comparisons between different histologic components in combined small cell lung cancer and non-small cell lung cancer. *Lung Cancer* 2018; 125: 282–290.
35. Byers LA, Diao L, Wang J, *et al.* An epithelial-mesenchymal transition gene signature predicts resistance to EGFR and PI3K inhibitors and identifies Axl as a therapeutic target for overcoming EGFR inhibitor resistance. *Clin Cancer Res* 2013; 19: 279–290.
36. Zhang YC, Chen ZH, Zhang XC, *et al.* Analysis of resistance mechanisms to abivertinib, a third-generation EGFR tyrosine kinase inhibitor, in patients with EGFR T790M-positive non-small cell lung cancer from a phase I trial. *EBioMedicine* 2019; 43: 180–187.
37. Solassol J, Vendrell JA, Senal R, *et al.* Challenging BRAF/EGFR co-inhibition in NSCLC using sequential liquid biopsies. *Lung Cancer* 2019; 133: 45–47.
38. Shaurova T, Zhang L, Goodrich DW, *et al.* Understanding lineage plasticity as a path to targeted therapy failure in EGFR-mutant non-small cell lung cancer. *Front Genet* 2020; 11: 281.